



HAL
open science

$\text{Ln}_3[\text{SiON}_3]\text{O}$ (Ln = La, Ce, Pr) – Three Oxonitridosilicate Oxides with Crystal Structures Derived from the Anti-Perovskite Structure Type

Juliane Kechele, Christian Schmolke, Saskia Lupart, Wolfgang Schnick

► **To cite this version:**

Juliane Kechele, Christian Schmolke, Saskia Lupart, Wolfgang Schnick. $\text{Ln}_3[\text{SiON}_3]\text{O}$ (Ln = La, Ce, Pr) – Three Oxonitridosilicate Oxides with Crystal Structures Derived from the Anti-Perovskite Structure Type. *Journal of Inorganic and General Chemistry / Zeitschrift für anorganische und allgemeine Chemie*, 2009, 636 (1), pp.176. 10.1002/zaac.200900274 . hal-00507773

HAL Id: hal-00507773

<https://hal.science/hal-00507773>

Submitted on 31 Jul 2010

HAL is a multi-disciplinary open access archive for the deposit and dissemination of scientific research documents, whether they are published or not. The documents may come from teaching and research institutions in France or abroad, or from public or private research centers.

L'archive ouverte pluridisciplinaire **HAL**, est destinée au dépôt et à la diffusion de documents scientifiques de niveau recherche, publiés ou non, émanant des établissements d'enseignement et de recherche français ou étrangers, des laboratoires publics ou privés.



**Ln₃[SiON₃]O (Ln = La, Ce, Pr) – Three Oxonitridosilicate
 Oxides with Crystal Structures Derived from the Anti-
 Perovskite Structure Type**

Journal:	<i>Zeitschrift für Anorganische und Allgemeine Chemie</i>
Manuscript ID:	zaac.200900274.R1
Wiley - Manuscript type:	Article
Date Submitted by the Author:	25-May-2009
Complete List of Authors:	Kechele, Juliane; Ludwig-Maximilians-Universitaet Muenchen, Department Chemie und Biochemie Schmolke, Christian; Ludwig-Maximilians-Universitaet Muenchen, Department Chemie und Biochemie Lupart, Saskia; Ludwig-Maximilians-Universitaet Muenchen, Department Chemie und Biochemie Schnick, Wolfgang; Ludwig-Maximilians-Universitaet Muenchen, Department Chemie und Biochemie
Keywords:	Magnetic properties, Oxonitridosilicate oxide, Solid-state NMR, Rietveld refinement, Structure elucidation



1
2
3
4
5
6
7
8
9
10
11
12
13
14
15
16
17
18 **Ln₃[SiON₃]O (Ln = La, Ce, Pr) – Three Oxonitridosilicate Oxides with**
19 **Crystal Structures Derived from the Anti-Perovskite Structure Type**
20
21
22
23
24
25
26
27
28

29 **Juliane A. Kechele, Christian Schmolke, Saskia Lupart, and Wolfgang Schnick ***
30
31

32 Department Chemie und Biochemie der Ludwig-Maximilians-Universität München
33
34

35
36 Received ...
37
38
39
40
41
42
43
44
45
46
47
48
49
50
51
52
53

54 * Prof. Dr. W. Schnick
55 Department Chemie und Biochemie
56 Lehrstuhl für Anorganische Festkörperchemie
57 Ludwig-Maximilians-Universität München
58 Butenandtstraße 5 – 13 (D)
59 D-81377 München, Germany
60 Fax: +49-(0)89-2180-77440
E-mail: wolfgang.schnick@uni-muenchen.de

Abstract

The oxonitridosilicate oxides $\text{Ln}_3[\text{SiON}_3]\text{O}$ with $\text{Ln} = \text{La}, \text{Ce}, \text{Pr}$ were obtained by high-temperature syntheses (1450 - 1600 °C) in a radio-frequency furnace. The crystal structures were determined from single-crystal X-ray diffraction data and confirmed by Rietveld refinements. The compounds $\text{Ln}_3[\text{SiON}_3]\text{O}$ crystallize in space group $I4/mcm$ ($\text{La}_3[\text{SiON}_3]\text{O}$: $a = 6.8224(10)$, $c = 11.074(2)$ Å, $Z = 4$; $R1 = 0.0240$; $\text{Ce}_3[\text{SiON}_3]\text{O}$: $a = 6.7233(10)$, $c = 11.069(2)$ Å, $Z = 4$, $R1 = 0.0234$; $\text{Pr}_3[\text{SiON}_3]\text{O}$: $a = 6.6979(9)$, $c = 11.005(2)$ Å, $Z = 4$; $R1 = 0.0156$) and they were found to be isotypic with $\text{Gd}_3[\text{SiON}_3]\text{O}$, whose structure derives from the anti-perovskite structure type. In the crystal there are elongated OLn_6 -octahedra which are interconnected through common vertices. In the cavities of this network there are exclusively non-condensed SiON_3 tetrahedra. ^{29}Si solid-state NMR investigations, lattice energy calculations (MAPLE) and EDX measurements confirmed the crystal structure and the chemical compositions. For $\text{Ce}_3[\text{SiON}_3]\text{O}$, magnetic susceptibility measurements were carried out and the paramagnetic behavior with an experimental magnetic moment of $2.2 \mu_B$ per cerium atom indicates Ce^{3+} .

Keywords

Magnetic properties; Oxonitridosilicate oxide; Rietveld refinement; Solid-state NMR; Structure elucidation

Introduction

In the literature there are multitudinous reports on varied possibilities for substitution and distortion in perovskite type materials.^[1] In this context, the oxonitridosilicate oxide $\text{Gd}_3[\text{SiON}_3]\text{O}$ ^[2] has been investigated which is isotypic to $\text{Ba}_3[\text{SiO}_4]\text{O}$ ^[3,4] and $\text{Cs}_3[\text{CoCl}_4]\text{Cl}$.^[5] All three compounds can be derived from the anti-perovskite structure type in a hierarchical sense with tetrahedral building blocks (SiON_3 , SiO_4 , CoCl_4) substituting the large alkaline earth ions in perovskite.

Oxonitridosilicates are intermediates between classical oxosilicates and nitridosilicates and can be formally derived by partial substitution of O for N. While oxygen in classical oxosilicates usually occur in a terminal $\text{O}^{[1]}$ or simply bridging $\text{O}^{[2]}$ function, nitrogen atoms can additionally act as a triply ($\text{N}^{[3]}$) or even quadruply ($\text{N}^{[4]}$) bridging atom, leading to a manifold of additional structural possibilities. Consequently, nitridosilicates exhibit a more

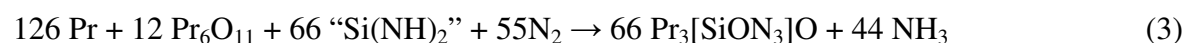
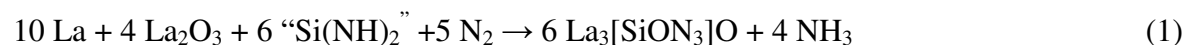
variable degree of condensation in the range $1 : 4 \leq \kappa \leq 3 : 4$ (i.e. the molar ration Si : (N,O)) as compared to classical oxosilicates ($1 : 4 \leq \kappa \leq 1 : 2$). Due to the enhanced connectivity of $N^{[3]}$ and even $N^{[4]}$ nitrogen atoms, new topological building blocks are possible. For example, in $BaYbSi_4N_7$ a “star-shaped” unit $[N^{[4]}(SiN_3)_4]$ has been observed for the first time.^[6] Here, the quadruply bridging nitrogen atom ($N^{[4]}$) adopts ammonium character. A further structural motif, which is unknown for oxosilicates so far, is the highly-condensed *dreier* ring layer.^[7] This kind of layer can be found in the layer oxosilicates $MSi_2O_2N_2$ ($M = Ca, Sr, Ba, Eu$)^[8-11] or it is part of the silicate framework (e.g. in $M_2Si_5N_8$ ^[12,13] ($M = Ca, Sr, Ba$), MSi_7N_{10} ($M = Sr, Ba$)).^[14,15] Most structures of (oxo)nitridosilicates analyzed so far, contained a highly condensed framework.^[16,17] However, the anionic part of the structure of $Gd_3[SiON_3]O$ contains exclusively non-condensed $SiON_3$ tetrahedra. Further examples for oxonitridosilicates with non-condensed silicate substructure are $Li_6[SiN_2O_2]$,^[18] $Ln_{10}[SiO_{3.67}N_{0.33}]_6O_2$ ($Ln = La, Nd, Sm, Gd$),^[19] $M_{10}[SiO_2N_2]_6O_2$ ($M = Ti, Ge$),^[19] and $LnEu[SiO_3N]$ ($Ln = La, Nd, Sm$).^[20]

In this contribution, we report on the syntheses, crystal structures and magnetic properties of $Ln_3[SiON_3]O$ with $Ln = La, Ce, Pr$. These compounds are isotypic to $Gd_3[SiON_3]O$, which has been described in the literature before.

Results and discussion

Syntheses and sample characterization

As exemplified by the synthesis of $Pr_3[SiON_3]O$, the compounds $Ln_3[SiON_3]O$ ($Ln = La, Ce, Pr$) can be obtained by various synthetic routes (cf. equation (1) – (5)) at temperatures ranging between 1450 and 1600 °C with varying purity degrees. The metals Ln (La, Ce, Pr), different Ln oxides, silicon diimide, and SiO_2 were used as starting materials for the syntheses. The oxidation state of the Ln in the starting material is apparently irrelevant. Starting from the respective metals leads to intermediate formation of the nitrides LnN ($Ln = La, Ce, Pr$).



The chemical composition and the phase purity of the samples were confirmed by EDX measurements and Rietveld refinements of the X-ray powder diffraction data (cf. Figure 1).

Crystal structure description

The structure of $\text{Ln}_3[\text{SiON}_3]\text{O}$ ($\text{Ln} = \text{La}, \text{Ce}, \text{Pr}$) is isotypic to $\text{Gd}_3[\text{SiON}_3]\text{O}$, which is derived from the anti-perovskite structure type.^[21] In Figure 2, the crystallographic relationship between the two structures is clarified using a group-subgroup scheme. Due to the hierarchical structural relation (SiON_3 units substitute for alkaline earth in the perovskite structure type) the complex SiON_3 tetrahedra have been approximated by the coordinates of their tetrahedral center (Si).

The crystal structure of the compounds consists of a framework which is built up of exclusively vertex-sharing OLn_6 octahedra ($\text{Ln} = \text{La}, \text{Ce}, \text{Pr}$). These octahedra are elongated along [001] and tilted as compared to the ideal cubic perovskite structure type (cf. Figure 3). The twisting is caused by electrostatic reasons or size effects, as the Ca atoms in the perovskite structure type are substituted by SiON_3 tetrahedra in $\text{Ln}_3[\text{SiON}_3]\text{O}$ ($\text{Ln} = \text{La}, \text{Ce}, \text{Pr}$). These SiON_3 tetrahedra are exclusively non-condensed and fill the voids of the OLn_6 octahedra framework. A differentiation of the O and N atoms was not possible by X-ray methods, as there is only one crystallographic position for these atoms belonging to the tetrahedra. Thus, the O and N atoms were distributed to the light atom positions on the basis of the crystal structure of the isotypic compound $\text{Gd}_3[\text{SiON}_3]\text{O}$. This distribution was corroborated by lattice energy calculations (MAPLE, Madelung part of lattice energy).^[21,22] The results of the calculations based on the O/N distribution in $\text{Gd}_3[\text{SiON}_3]\text{O}$ are summarized in Table 1.

The distances Si-(O,N) (cf. Table 2) are in the typical range for terminal bonds Si-(O,N) in oxonitridosilicates (cf. $\text{La}_{16}[\text{Si}_8\text{N}_{22}][\text{SiON}_3]_2$: 1.689(5) - 1.743(8) Å;^[25] $\text{Ln}_{10}[\text{Si}_{10}\text{O}_9\text{N}_{17}]\text{X}$: 1.664(4) - 1.709(7) Å ($\text{Ln} = \text{Ce}, \text{X} = \text{Br}$), 1.666(3) - 1.713(5) Å ($\text{Ln} = \text{Nd}, \text{X} = \text{Br}$), 1.665(3) - 1.718(5) Å ($\text{Ln} = \text{Nd}, \text{X} = \text{Cl}$);^[26] $\text{Pr}_{10}[\text{Si}_{10-x}\text{Al}_x\text{O}_{9+x}\text{N}_{17-x}]\text{Cl}$ ($x \approx 1$): 1.674(7) - 1.739(6) Å).^[27] The angles $\text{N/O}(1)^{[1]}-\text{Si}(1)-\text{N/O}(1)^{[1]}$ (cf. Table 2) are close to the regular tetrahedral angle.

The structures of $\text{Ln}_3[\text{SiON}_3]\text{O}$ ($\text{Ln} = \text{La}, \text{Ce}, \text{Pr}$) contain two crystallographically independent Ln^{3+} sites, which are surrounded by eight and ten (N,O) atoms, respectively (cf. Figure 4). The distances $\text{Ln}-(\text{N},\text{O})$ ($\text{Ln} = \text{La}, \text{Ce}, \text{Pr}$) are listed in Table 2. Some distances $\text{Ln}(2)^{[8]}-(\text{N},\text{O})$ are slightly shorter than the smallest sum of the ionic radii ($\text{La}^{[8]}-\text{O}$: 2.56 Å; $\text{La}^{[8]}-\text{N}$: 2.62 Å; $\text{Ce}^{[8]}-\text{O}$: 2.54 Å; $\text{Ce}^{[8]}-\text{N}$: 2.60 Å; $\text{Pr}^{[8]}-\text{O}$: 2.53 Å; $\text{Pr}^{[8]}-\text{N}$: 2.59 Å)^[28] but the distances are in the same range than in other well characterized oxonitrido(alumo)silicates (e.g.: $\text{La}_4\text{Si}_2\text{O}_7\text{N}_2$: $\text{La}-(\text{O},\text{N})$ 2.298(6) - 2.903(5) Å;^[29] $\text{Ce}_{10}[\text{Si}_{10}\text{O}_9\text{N}_{17}]\text{Br}$: $\text{Ce}-(\text{O},\text{N})$ 2.409(4)

1
2
3 – 2.7465(7) Å, Ce-N 2.447(7) – 3.016(5) Å,^[26] Pr₁₀[Si_{10-x}Al_xO_{9+x}N_{17-x}]Cl (x ≈ 1): Pr-(O,N)
4 2.390(4) – 2.7465(7) Å, Pr-N 2.439(7) – 3.08(5) Å.^[27]
5
6

7 The anisotropic displacement parameters of the Ln(1) site are larger by the factor of about 2-3
8 in comparison with the values of the Ln(2) site (Ln = La, Ce, Pr). Most probably, local
9 deviations from the special site of Ln(1) causes the increase of the parameters. This effect was
10 also observed for Gd₃[SiON₃]O.^[2]
11
12

13 Furthermore, the displacement ellipsoid of O(2) is elongated, which is presumably due to the
14 deformation of the OLn₆ octahedra (Ln = La, Ce, Pr), mentioned above. Therefore, a splitting
15 of this site was assumed at lower temperatures analogously with the Gd containing
16 compound. A crystal structure investigation for Ce₃[SiON₃]O at 130 K confirmed this
17 assumption.
18
19
20
21
22

23 ²⁹Si solid-state NMR

24 The ²⁹Si solid-state NMR spectrum of La₃[SiON₃]O shows one broad signal peaking at -
25 56.2 ppm with a full width at half maximum of 8 ppm (cf. Figure 5) This broadness of the
26 signal is caused by the quadrupole momentum of the La atoms. The signal corresponds to
27 SiON₃ tetrahedra as evidenced by comparable shifts in La containing oxonitridoalumosilicate
28 glasses (-54.4 and -56.0 ppm). For these compounds also the shifts for SiN₄ (-43.3 and -
29 46.9 ppm) and SiN₂O₂ (-64.0, -62.5 and -60.9 ppm) were reported, which are not in the same
30 range.^[30] Therefore, the NMR results corroborate that La₃[SiON₃]O exhibits exclusively
31 SiON₃ tetrahedra as evidenced by lattice energy calculations (MAPLE).
32
33
34
35
36
37
38
39
40
41

42 *Magnetical behavior*

43 In the insert of Figure 6 the isothermal magnetization (at 2 and 300 K) of Ce₃[SiON₃]O is
44 depicted. Below the Curie-temperature T_C ≈ 7 K, a ferromagnetic ordering was observed. The
45 saturation magnetization converges to a value of 3 μ_B per formula unit, which is in accordance
46 with three Ce³⁺ ions per formula unit.
47
48
49

50 The temperature dependence of the reciprocal magnetic susceptibility is shown in Figure 6.
51 **The bending of the reciprocal susceptibility curve is most probably caused by an amorphous**
52 **by-product, which could not be determined by powder** diffraction. Due to crystal field effects
53 a certain deviation from Curie-Weiss behavior is observed. Therefore, the data between 200
54 and 300 K were fitted with an extended Curie-Weiss equation $\chi_m = \chi_0 + C/(T - \theta)$, which
55 results in an effective magnetic moment of 2.2 μ_B per Ce. The temperature independent part
56 of the susceptibility χ_0 is comparatively large as the crystal field effects are neglected and has
57
58
59
60

1
2
3 no physical meaning. The magnetic moment is slightly below the theoretical value for free
4
5 Ce^{3+} ($2.54 \mu_{\text{B}}$). However, most of the experimentally determined values for Ce^{3+} containing
6
7 compounds have been reported between 2.3 and $2.5 \mu_{\text{B}}$.^[31] Therefore, the measurements
8
9 corroborate occurrence of solely Ce^{3+} in $\text{Ce}_3[\text{SiON}_3]\text{O}$.

10 11 ***Comparison of $\text{Ln}_3[\text{SiON}_3]\text{O}$ with other A_3BX_5 phases***

12 The *a/c* ratio of the compounds $\text{Ln}_3[\text{SiON}_3]\text{O}$ ($\text{Ln} = \text{La, Ce, Pr, Gd}$) decreases between La and
13
14 Gd according to the ionic radii. For the Ce and Pr containing compounds the values are
15
16 identical within the margin of error, as the two ions have almost identical radii. However, this
17
18 trend could not be observed for the lattice parameters of the compounds. Therefore, the
19
20 correlation between the ratio *a/c* and the ionic radii is probably caused by an anisotropic
21
22 framework folding mechanism, which modulates the cavities. The same trend was observed
23
24 for the deviation of the OLn_6 units from regular octahedral symmetry ($\text{Ln} = \text{La, Ce, Pr, Gd}$)
25
26 (cf. Table 3). A correlation between the *a/c* ratio and the distortion of the octahedra could also
27
28 be observed for isotypic compounds $\text{Cs}_3[\text{CoCl}_4]\text{Cl}$ ^[5] and $\text{Ba}_3[\text{SiO}_4]\text{O}$.^[3,4] However, the tilting
29
30 angle ξ is independent from the *a/c* ratio of the compounds. For $\text{Ln}_3[\text{SiON}_3]\text{O}$ ($\text{Ln} = \text{La, Ce,}$
31
32 Pr, Gd) the values are in the same range, but there is no trend observable according to the
33
34 ionic radii.

35 36 37 **Conclusions**

38 In the last years, (oxo)nitridosilicates have received remarkable attention in materials science,
39
40 as these compounds are both thermally and chemically very stable. With the syntheses of
41
42 $\text{Ln}_3[\text{SiON}_3]\text{O}$ ($\text{Ln} = \text{La, Ce, Pr}$), oxonitridosilicates with non-condensed tetrahedra could be
43
44 obtained, although this group of compounds has a stronger tendency to form condensed
45
46 networks than classical oxosilicates. Due to the non-condensed silicate substructure, the
47
48 compounds are air- and water sensitive.

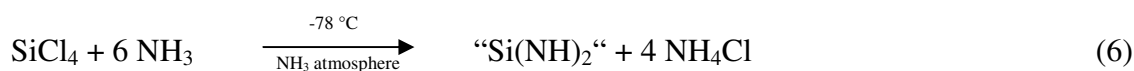
49 Although it was possible to investigate the distribution O/N for the La containing compound
50
51 by means of solid-state NMR measurements, it would be interesting to precisely determine
52
53 the distribution using neutron diffraction. However, the available single crystals are yet too
54
55 small for single-crystal neutron diffraction. Moreover powder data are most probably not
56
57 conclusive enough, as one crystallographic light atom position has to be occupied statistically
58
59 with both nitrogen and oxygen atoms and there was no indication for a decrease in symmetry.
60

Experimental part

Syntheses

Synthesis of silicon diimide “Si(NH)₂”

Instead of the relatively unreactive Si₃N₄ silicon diimide was used as starting material. Previous syntheses of several (oxo)nitridosilicates and oxonitridoalumosilicates showed, that “Si(NH)₂” is well suited as starting material.^[16,17,32] According to equation 1 and 2, the X-ray amorphous and relatively undefined compound was obtained by ammonolysis of SiCl₄ (> 98%, Merck, Darmstadt), followed by a thermal treatment at 600 °C under an atmosphere of pure NH₃.



Synthesis of La₃[SiON₃]O

For the synthesis of La₃[SiON₃]O La (231.5 mg, 1.67 mmol, 99.9 %, Smart Elements) as small pieces, silicon diimide (53.8 mg, 0.25 mmol) and La₂O₃ (217.2 mg, 0.67 mmol, 99.999 %, Chempur) were mixed in an agate mortar and filled in a tungsten crucible under argon atmosphere in a glove box (Unilab, MBraun, O₂ ≤ 1 ppm, H₂O ≤ 1 ppm). Under purified N₂, the crucible was heated to 1600 °C within 1 h in the reactor of a radio-frequency furnace^[32] and this maximum temperature was kept for 10 h. Subsequently, the crucible was cooled down to 900 °C with a rate of about 16 °C h⁻¹ before quenching to room temperature by switching off the furnace. The sample contains exclusively La₃[SiON₃]O as green-yellow crystals.

Synthesis of Ce₃[SiON₃]O

Ce₃[SiON₃]O was synthesized starting from Ce (280.2 mg, 2.0 mmol, 99.9%, Smart Elements) as small pieces, CeO₂ (172.1 mg, 1.0 mmol, 99.99 %, Chempur) and silicon diimide (53.8 mg, 0.25 mmol). After thoroughly mixing the starting materials in an agate mortar, the mixture was filled in a tungsten crucible under argon atmosphere in a glove box (Unilab, MBraun, O₂ ≤ 1 ppm, H₂O ≤ 1 ppm). The crucible was heated in a radio-frequency furnace analogously with the synthesis of the La containing compound. Ce₃[SiON₃]O was obtained without any by-products as dark-red crystals.

Synthesis of Pr₃[SiON₃]O

Pr₃[SiON₃]O was obtained with varying degrees of purity by diverse synthetic routes using different starting materials. For example, Pr₄Si₂O₇N₂ [33] or PrN [34] were observed as by-products. For all syntheses, the starting materials were thoroughly mixed in an agate mortar in a glove box (Unilab, MBraun, O₂ ≤ 1 ppm, H₂O ≤ 1 ppm) and subsequently heated in a tungsten crucible in a radio-frequency furnace under purified N₂.

One possibility to synthesize the compound starts from metallic Pr (178.8 mg, 1.27 mmol, 99.9%, Chempur, Karlsruhe) as small pieces, silicon diimide (37.0 mg, 0.17 mmol) and Pr₆O₁₁ (110.1 mg, 1.1 mmol, > 99.9 %, Auer Remy, Hamburg). The mixture was heated to 950 °C within 5 min and kept for 25 min. Afterwards the temperature was increased to 1450 °C with a rate of about 42 °C h⁻¹ and kept at that temperature for 8 h. Subsequently, the crucible was cooled down to 750 °C with a rate of about 140 °C h⁻¹ before switching off the furnace.

For an alternative synthetic route Pr (211.3 mg, 1.5 mmol, 99.9%, Chempur, Karlsruhe) as small pieces and SiO₂ (30.4 mg, 0.5 mmol, ≥ 99.8%, Degussa, Frankfurt/Main) were used as starting materials. The heating program is similar to the program for the synthesis of La₃[SiON₃]O, but as maximum temperature 1550 °C was chosen.

Pr₃[SiON₃]O was also observed as product of the reaction between Pr (169.1 mg, 1.2 mmol, 99.9%, Chempur, Karlsruhe) and silicon diimide (53.8 mg; 0.25 mmol). Probably, the starting materials were contaminated with oxygen in the latter case. The crucible was heated with the same temperature program as used for the syntheses of Ln₃[SiON₃]O (Ln = La, Ce).

Chemical Analyses

Elemental analyses on selected crystals were performed for all compounds by energy dispersive X-ray spectroscopy (EDX) using a JSM-6500F scanning electron microscope (Jeol) with a Si/Li EDX detector (Oxford Instruments, model 7418). The measurements indicate a molar ratio Ln/Si = 3 : 1 (Ln = La, Ce, Pr), which corroborates the formation of Ln₃[SiON₃]O (Ln = La, Ce, Pr). The determined compositions are in accordance with the structure model within the typical error ranges, as the result for Pr₃[SiON₃]O demonstrates (calc. (at%): Pr 33, Si 11, N 33, O 22; found (at%): Pr 30, Si 9, N 36 O 24).

Single-crystal X-ray analysis

1
2
3 Single crystals of $\text{Ln}_3[\text{SiON}_3]\text{O}$ ($\text{Ln} = \text{La}, \text{Ce}, \text{Pr}$) were isolated, enclosed in glass capillaries
4 (0.2 mm), and sealed under argon atmosphere. Initially, the crystals were examined by Laue
5 photographs recorded on a Bueger camera equipped with an image plate system. Single-
6 crystal X-ray data of all compounds were collected at room temperature on a STOE IPDS I
7 diffractometer (Stoe and Cie GmbH; Darmstadt) with Mo-K_α radiation (0.71073 Å, graphite
8 monochromator). The structures were solved by direct methods and refined after a numerical
9 or semiempirical absorption correction of the diffraction data.^[35,36] The SHELX suite of
10 programs was used for all calculations.^[37,38] Details concerning the data collection and
11 refinements are summarized in Table 4. Further details of the crystal-structure investigations
12 may be obtained from the Fachinformationszentrum Karlsruhe, D-6344 Eggenstein-
13 Leopoldshafe, Germany, on quoting the depository numbers CSD-420626 ($\text{Ln} = \text{La}$), 420627
14 ($\text{Ln} = \text{Ce}$), and 420628 ($\text{Ln} = \text{Pr}$). The atomic coordinates, the equivalent displacement
15 parameters, and the site occupancy factors of the three compounds are listed in Table 5 - 7
16
17
18
19
20
21
22
23
24
25
26
27

28 *X-ray powder diffraction*

29
30 X-ray powder diffraction data were collected on a STOE STADI P diffractometer with Mo-
31 K_α radiation (0.71073 Å) in Debye-Scherrer geometry. The samples were enclosed in silica
32 tubes (0.2 mm), and sealed under argon atmosphere. For pattern fitting (LeBail algorithm) and
33 Rietveld refinement, the GSAS program package^[39] was used. The results of the single-
34 crystal X-ray analyses were used as starting models. The crystallographic data and details of
35 the Rietveld refinements are given in Table 8. The isotropic displacement parameters were
36 constrained to be equal for both the two Ln sites ($\text{Ln} = \text{La}, \text{Ce}, \text{Pr}$) and the N and O positions,
37 respectively. Furthermore, the (N,O) site occupancies were fixed. The analyses of the data
38 unequivocally confirmed the purity of the compounds.
39
40
41
42
43
44
45
46
47

48 *Solid-state NMR*

49
50 Solid-state NMR measurements have been performed on a Bruker Avance DSX 500
51 spectrometer with an external magnetic field of 11.75 T for $\text{La}_3[\text{SiON}_3]\text{O}$. The ^{29}Si -1D-MAS
52 spectra were recorded with direct excitation using a commercial triple resonance MAS probe,
53 which was equipped with a rotor made of ZrO_2 (diameter: 4 mm). A repetition delay of 4096 s
54 ($> 3T_1$) and a rotation frequency of 9 kHz were chosen. The 90° impulse length was 2.5 μs.
55 The given chemical shift values refer to TMS as external chemical shift reference.
56
57
58
59
60

Magnetic Measurements

Magnetic properties of $\text{Ce}_3[\text{SiON}_3]\text{O}$ were measured utilizing a SQUID magnetometer (MPMS-XL Quantum Design Inc.). The sample was inserted in a capsule as fine ground powder which was fitted onto a straw of known diamagnetism. The magnetic susceptibility of the sample was collected between 2 and 300 K with magnetic flux densities up to 0.9 T. The obtained data were corrected for diamagnetic contributions of the capsule, the straw, and the sample using diamagnetic increments and analyzed with a modified Curie-Weiss law $\chi_m = \chi_0 + C/(T - \theta)$. From the Curie constant C, the effective magnetic moment per formula unit is calculated using the spin-only approximation.

Supporting Information: Anisotropic displacement parameters for the three compounds

$\text{Ln}_3[\text{SiON}_3]\text{O}$ with Ln = La, Ce, Pr..

Acknowledgements: The authors thank Dr. Oliver Oeckler and Thomas Miller for the collection of the single-crystal data as well as Christian Minke for performing the EDX measurements. The investigations of the magnetical behavior by Prof. Dr. Dirk Johrendt and Daniel Bichler are gratefully acknowledged. Furthermore the authors thank Dr. Jörn Schmedt auf der Günne and Christian Minke for the solid-state NMR measurement. This work was financially supported by the Fonds der Chemischen Industrie (FCI).

Table 1 Results of the MAPLE calculations [kJ/mol] for $\text{Ln}_3[\text{SiON}_3]\text{O}$ ($\text{Ln} = \text{La}, \text{Ce}, \text{Pr}$) based on the O/N distribution in $\text{Gd}_3[\text{SiON}_3]\text{O}$. Δ = difference.

	Ln^{3+}	Si^{4+}	$(\text{N},\text{O})^{2.75-}$	O^{2-}	Total	Δ
	MAPLE					
La:	3957; 4215	10021	4029	1942	40466	0.9
Ce:	4010; 4275	9924	4058	1943	40656	0.4
Pr:	4022; 4295	10000	4078	1955	40878	0.5
Total MAPLE (3 LaN + SiO ₂): 40089 kJ/mol						
Total MAPLE (3 CeN + SiO ₂): 40499 kJ/mol						
Total MAPLE (3 PrN + SiO ₂): 40670 kJ/mol						
Typical partial MAPLE values [kJ/mol]: La ³⁺ : 3500 - 5000; Ce ³⁺ : 3800 - 4800; Pr ³⁺ : 3800 - 4500; Si ⁴⁺ : 9000 - 10200; O ²⁻ : 2000 - 2800; (N,O) ^{2.75-} : 4000 - 5200. ^[23,24]						

Table 2 Selected interatomic distances (Å) and angles (°) for Ln₃[SiN₃O]O (Ln = La, Ce, Pr). Standard deviations are given in parentheses.

		La	Ce	Pr
Ln(1)-O(2) ^[0]	(2x)	2.7684(5)	2.7671(5)	2.7513(5)
Ln(1)-N/O(1) ^[1]	(8x)	2.858(4)	2.818(3)	2.8078(19)
Ln(2)-N/O(1) ^[1]	(2x)	2.450(6)	2.411(5)	2.402(3)
Ln(2)-O(2) ^[0]	(2x)	2.5157(4)	2.4804(4)	2.4701(3)
Ln(2)-N/O(1) ^[1]	(4x)	2.734(5)	2.712(4)	2.699(3)
Si(1)-N/O(1) ^[1]	(4x)	1.728(6)	1.736(5)	1.724(3)
N/O(1) ^[1] -Si(1)-N/O(1) ^[1]		101.5(4), 113.6(2)	101.1(3), 113.79(17)	101.1(2), 113.83(13)

Table 3 Comparison of the relevant data of isotypic compounds $\text{Ln}_3[\text{SiON}_3]\text{O}$, $\text{Ba}_3[\text{SiO}_4]\text{O}$, $\text{Cs}_3[\text{CoCl}_4]\text{Cl}$ with perovskite.

compound	<i>a/c</i> ratio	angle $\xi / ^\circ$	deviation from the average X-M distance
$\text{Gd}_3[\text{SiON}_3]\text{O}$	0.603(1)	16.47(1)	5.3 % (X = O, M = Gd)
$\text{Pr}_3[\text{SiON}_3]\text{O}$	0.609(2)	16.53(1)	4.9 % (X = O, M = Pr)
$\text{Ce}_3[\text{SiON}_3]\text{O}$	0.607(2)	16.60(1)	4.9 % (X = O, M = Ce)
$\text{La}_3[\text{SiON}_3]\text{O}$	0.616(2)	16.50(1)	4.3 % (X = O, M = La)
$\text{Cs}_3[\text{CoCl}_4]\text{Cl}$	0.635	19.34	2.4 % (X = Cl, M = Cs)
$\text{Ba}_3[\text{SiO}_4]\text{O}$	0.651	14.96	2.2 % (X = O, M = Ba)
$\text{Ca}[\text{TiO}_3]$	$2^{-1/2}$	0	none (X = Ti, M = O)

Table 4 Crystallographic data and details of the refinement procedures for $\text{Ln}_3[\text{SiON}_3]\text{O}$ (Ln = La, Ce, Pr). Standard deviations are given in parentheses.

Formula	$\text{La}_3[\text{SiON}_3]\text{O}$	$\text{Ce}_3[\text{SiON}_3]\text{O}$	$\text{Pr}_3[\text{SiON}_3]\text{O}$
Molar mass / g mol^{-1}	518.85	522.48	524.85
Crystal system		tetragonal	
Space group		$I4/mcm$ (no. 140)	
Cell parameters / Å	$a = 6.8224(10)$	$a = 6.7233(10)$	$a = 6.6979(9)$
	$c = 11.074(2)$	$c = 11.069(2)$	$c = 11.005(2)$
Cell volume / Å^3	515.43(15)	500.33(14)	493.72(14)
Formula units / cell		$Z = 4$	
X-ray density / g cm^{-3}	6.686	6.936	7.061
Abs. coefficient / mm^{-1}	24.550	26.969	29.275
F(000)	888	900	912
Crystal size / mm^3	0.07 x 0.06 x 0.04	0.08 x 0.05 x 0.04	0.06 x 0.05 x 0.04
Diffractometer		STOE IPDS	
Radiation, monochromator		Mo- K_α ($\lambda = 0.71073\text{Å}$), graphite	
Temperature / K	293(2)	293(2)	293(2)
2θ range / $^\circ$	$4.22 \leq \theta \leq 28.47$	$3.68 \leq \theta \leq 29.98$	$3.70 \leq \theta \leq 30.22$
Total no. of reflections	2016	2409	2435
Independent reflections	195	218	220
Observed reflections	164	200	202
Absorption correction	numerical	semiempirical (from equivalents)	numerical
Refined parameters	18	18	18
GOF	1.050	1.152	1.077
R -values [$I > 2\sigma(I)$]	$R1 = 0.0182$	$R1 = 0.0208$	$R1 = 0.0131$
	$wR2 = 0.0363$	$wR2 = 0.0430$	$wR2 = 0.0276$
all data	$R1 = 0.0240$	$R1 = 0.0234$	$R1 = 0.0156$
	$wR2 = 0.0370$	$wR2 = 0.0435$	$wR2 = 0.0281$
Max. / min. residual electron density / e Å^{-3}	-0.892; 0.962	-1.311; 1.920	-0.763; 0.771

Table 5 Atomic coordinates, equivalent displacement parameters, and site occupancy factors for $\text{La}_3[\text{SiN}_3\text{O}]\text{O}$. (T = 293 K). Standard deviations are given in parentheses.

Atom	Wykoff symbol	s.o.f.	x	y	z	U_{eq}
La(1)	4a	1	0	0	1/4	0.0215(3)
La(2)	8h	1	0.67593(5)	0.17593(5)	0	0.0119(2)
Si(1)	4b	1	0	1/2	1/4	0.0092(7)
N/O(1)	16i	0.75; 0.25	0.1387(6)	0.6387(6)	0.1512(6)	0.0179(11)
O(2)	4c	1	0	0	0	0.024(3)

Table 6 Atomic coordinates, equivalent displacement parameters, and site occupancy factors for Ce₃[SiN₃O]O. (T = 293 K). Standard deviations are given in parentheses.

Atom	Wykoff symbol	s.o.f.	x	y	z	U _{eq}
Ce(1)	4a	1	0	0	¼	0.0143(3)
Ce(2)	8h	1	0.67548(4)	0.17548(4)	0	0.0059(3)
Si(1)	4b	1	0	1/2	¼	0.0057(8)
N/O(1)	16i	0.75; 0.25	0.1410(6)	0.6410(6)	0.1504(4)	0.0105(11)
O(2)	4c	1	0	0	0	0.021(3)

Table 7 Atomic coordinates, equivalent displacement parameters, and site occupancy factors for Pr₃[SiN₃O]O. (T = 293 K). Standard deviations are given in parentheses.

Atom	Wykoff symbol	s.o.f.	x	y	z	<i>U</i> _{eq}
Pr(1)	4a	1	0	0	¼	0.01389(15)
Pr(2)	8h	1	0.67581(3)	0.17581(3)	0	0.00488(13)
Si(1)	4b	1	0	1/2	¼	0.0039(4)
N/O(1)	16i	0.75; 0.25	0.1405(4)	0.6405(4)	0.1504(3)	0.0125(6)
O(2)	4c	1	0	0	0	0.0233(16)

Table 8 Crystallographic data of $\text{Ln}_3[\text{SiN}_3\text{O}]\text{O}$ derived from Rietveld refinement of X-ray data. Standard deviations are given in parentheses.

Formula	$\text{La}_3[\text{SiN}_3\text{O}]\text{O}$	$\text{Ce}_3[\text{SiN}_3\text{O}]\text{O}$	$\text{Pr}_3[\text{SiN}_3\text{O}]\text{O}$
Crystal system		tetragonal	
Space group		$I4/mcm$ (no. 140)	
Lattice parameters / Å	$a = 6.82172(17)$	$a = 6.72040(10)$	$a = 6.68498(8)$
	$c = 11.0981(3)$	$c = 11.0544(2)$	$c = 10.99356(17)$
Cell volume / Å ³	516.46(4)	499.26(2)	491.291(17)
Formula units / cell		$Z = 4$	
Radiation		Mo- K_α ($\lambda = 0.70933\text{Å}$)	
Profile range / °	$2 \leq 2\theta \leq 50$	$2 \leq 2\theta \leq 60$	$2 \leq 2\theta \leq 60$
No. of data points	4800	5790	5500
Observed reflections	142	218	215
No. of refined parameters	61	60	61
R_p / wR_p	0.0990 / 0.1325	0.0538 / 0.0716	0.0466 / 0.0617
R_{F}^2	0.0753	0.0406	0.0458
GOF	0.97	1.36	1.16
Reduced χ^2	0.936	1.842	1.348

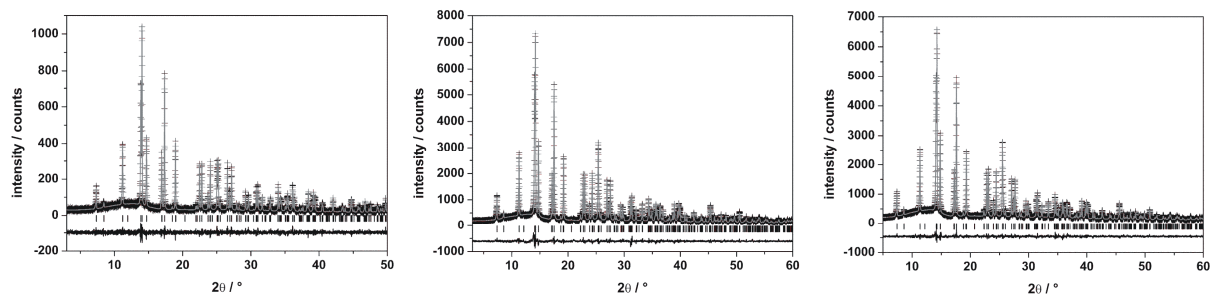


Fig. 1 Observed (crosses) and calculated (line) X-ray powder diffraction patterns as well as difference profile for the Rietveld refinement of Ln₃[SiON₃]O (left: La₃[SiON₃]O; middle: Ce₃[SiON₃]O; right: Pr₃SiON₃O).

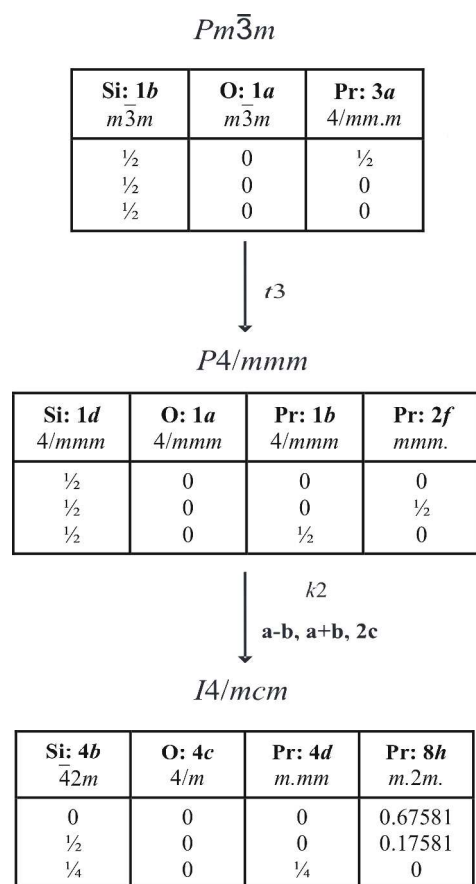


Fig. 2 Crystallographic group-subgroup relation (*Bärnighausen tree*)^[40] between $\text{Pr}_3[\text{SiON}_3]\text{O}$ and the perovskite structure type.

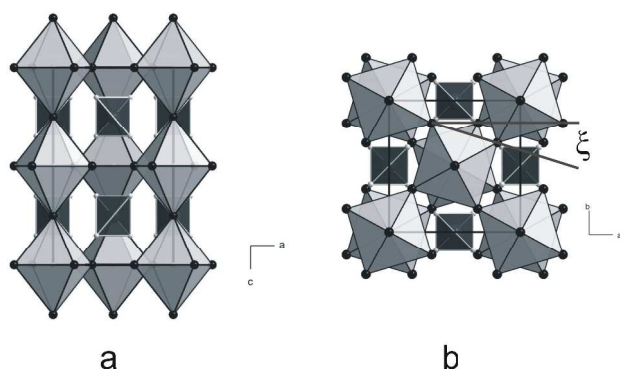


Fig. 3a: Structure of $\text{Ln}_3[\text{SiON}_3]\text{O}$ ($\text{Ln} = \text{La}, \text{Ce}, \text{Pr}$) viewed along $[010]$. **b:** Structure viewed along $[001]$; the twisting angle ξ is indicated. The OLn_6 octahedra are depicted light gray, the SiON_3 tetrahedra dark gray. The black spheres symbolize Ln^{3+} atoms.

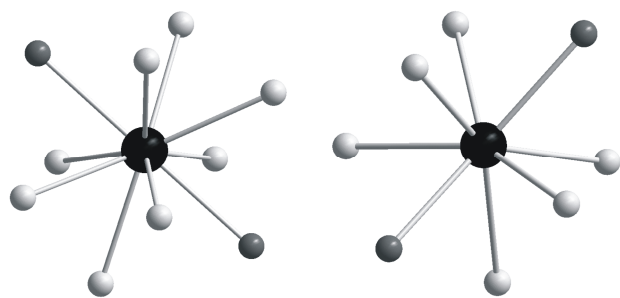


Fig. 4 Coordination spheres of the Ln^{3+} ions (left: Ln(1); right: Ln(2)) (Ln = La, Ce, Pr). (Ln: black; O: light gray; (N,O): dark gray).

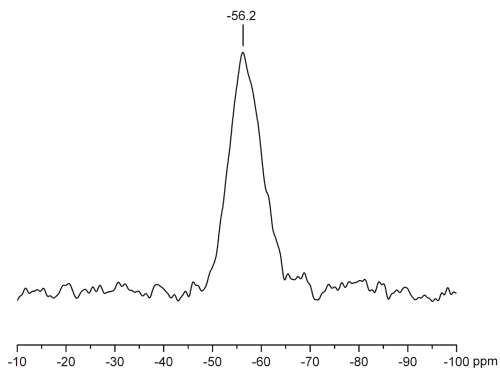


Fig. 5: ^{29}Si solid-state MAS NMR of $\text{La}_3[\text{SiON}_3]\text{O}$.

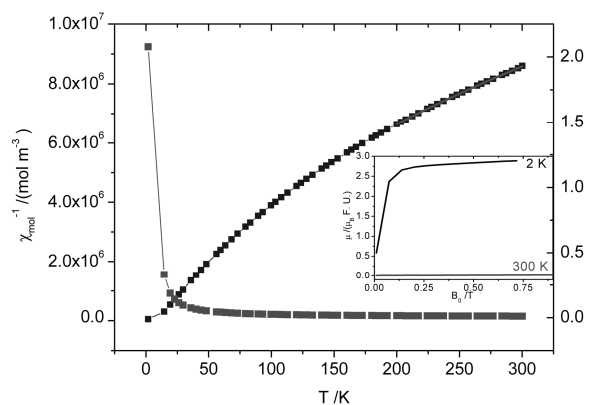


Fig. 6: Temperature dependence of the reciprocal susceptibility (black squares) and the susceptibility (gray squares) of $\text{Ce}_3[\text{SiON}_3]\text{O}$. Insert: Magnetization of $\text{Ce}_3[\text{SiON}_3]\text{O}$ as a function of varying field at different temperatures.

References

- [1] O. Bock, U. Müller, *Acta Crystallogr. B* **2002**, 58, 594.
- [2] H. A. Höpfe, G. Kotzyba, R. Pöttgen, W. Schnick, *J. Solid State Chem.* **2002**, 167, 393.
- [3] E. Tillmanns, H.-P. Grosse, *Acta Crystallogr. B.* **1978**, 34, 649.
- [4] M. Mansmann, *Z. Anorg. Allg. Chem.* **1965**, 339, 52.
- [5] H. M. Powell, A. F. Wells, *J. Chem. Soc.* **1935**, 359.
- [6] H. Huppertz, W. Schnick, *Angew. Chem.* **1996**, 108, 2115; *Angew. Chem. Int. Ed. Engl.* **1996**, 35, 1983.
- [7] A *dreier* ring can be described as a six-membered ring with *three* tetrahedral centers (e.g. Si) and *three* electronegative atoms (e.g. N), for example. (F. Liebau, *Structural Chemistry of Silicates*, Springer, Berlin, **1985**).
- [8] H. A. Höpfe, F. Stadler, O. Oeckler, W. Schnick, *Angew. Chem.* **2004**, 116, 5656; *Angew. Chem. Int. Ed.* **2004**, 43, 5540.
- [9] O. Oeckler, F. Stadler, T. Rosenthal, W. Schnick, *Solid State Sci.* **2007**, 9, 205.
- [10] J. A. Kechele, O. Oeckler, F. Stadler, W. Schnick, *Solid State Sci.* **2009**, 11, 537.
- [11] F. Stadler, O. Oeckler, H. A. Höpfe, M. H. Möller, R. Pöttgen, B. D. Mosel, P. Schmidt, V. Duppel, A. Simon, W. Schnick, *Chem. Eur. J.* **2006**, 12, 6984.
- [12] T. Schlieper, W. Schnick, *Z. Anorg. Allg. Chem.* **1995**, 621, 1037.
- [13] T. Schlieper, W. Milius, W. Schnick, *Z. Anorg. Allg. Chem.* **1995**, 621, 1380.
- [14] G. Pilet, H. A. Höpfe, W. Schnick, S. Esmaeilzadeh, *Solid State Sci.* **2005**, 7, 391.
- [15] H. Huppertz, W. Schnick, *Chem. Eur. J.* **1997**, 3, 249.
- [16] W. Schnick, H. Huppertz, *Chem. Eur. J.* **1997**, 3, 679.
- [17] W. Schnick, T. Schlieper, H. Huppertz, K. Köllisch, M. Orth, R. Bettenhausen, B. Schwarze, R. Lauterbach, *Phosphorus Sulfur Silicon Relat. Elem.* **1997**, 124/125, 163.
- [18] S. Podsiadlo, *J. Therm. Anal.* **1987**, 32, 771.
- [19] J. Guyader, F. F. Grekov, R. Marchand, J. Lang, *Rev. Chim. Miner.* **1978**, 15, 431.
- [20] R. Marchand, *C. R. Acad. Sci., Ser. IIC: Chim.* **1976**, 283, 281.
- [21] R. Hoppe, *Angew. Chem.* **1966**, 78, 52; *Angew. Chem. Int. Ed. Engl.* **1966**, 5, 95.
- [22] R. Hoppe, *Angew. Chem.* **1970**, 82, 7; *Angew. Chem. Int. Ed. Engl.* **1970**, 9, 25.
- [23] H. A. Höpfe, *PhD Thesis*, University of Munich, **2003**.
- [24] K. Köllisch, *PhD Thesis*, University of Munich, **2001**.
- [25] C. Schmolke, S. Lupart, W. Schnick, *Solid State Sci.* **2009**, 11, 305.
- [26] A. Lieb, W. Schnick, *J. Solid State Chem.* **2005**, 178, 3323.
- [27] A. Lieb, R. Lauterbach, W. Schnick, *Z. Anorg. Allg. Chem.* **2006**, 632, 313.
- [28] R. D. Shannon, *Acta Crystallogr. A* **1976**, 32, 751.
- [29] J. Takahashi, H. Yamane, N. Hirosaki, Y. Yamamoto, T. Suehiro, T. Kamiyama, M. Shimada, *Chem. Mater.* **2003**, 15, 1099.

- 1
2
3 [30] E. Leonova, A. S. Hakeem, K. Jansson, B. Stevansson, Z. Shen, J. Grins, S. Esmailzadeh, M,
4 Edén, *J. Non-Cryst. Solids* **2008**, 354, 49.
5
6 [31] H. Lueken, *Magnetochemie*, Teubner, Stuttgart, **1999**.
7
8 [32] W. Schnick, H. Huppertz, R. Lauterbach, *J. Mater. Chem.* **1999**, 9, 289.
9
10 [33] O. Greis, R. Ziel, B. Breidenstein, A. Haase, T. Petzel, *J. Alloys Compds.* **1994**, 216, 255.
11 [34] B. Iandelli, *Accademia Nazionale dei Lincei* **1937**, 25, 129.
12 [35] *X-Red 32*, Version 1.31, **2005**, STOE and Cie GmbH, Darmstadt.
13 [36] *X-SHAPE*, Version 2.07, **2005**, STOE and Cie GmbH, Darmstadt.
14 [37] G. M. Sheldrick, *Acta Crystallogr. A* **2008**, 64, 112.
15 [38] L. J. Farrugia, *J. Appl. Crystallogr.* **1999**, 32, 837.
16 [39] A. C. Larson, R. B. von Dreele, *GSAS – General Structure Analysis System*, Los Alamos, USA,
17 **1998**.
18 [40] U. Müller, *Z. Anorg. Allg. Chem.* **2004**, 630, 1519.
19
20
21
22
23
24
25
26
27
28
29
30
31
32
33
34
35
36
37
38
39
40
41
42
43
44
45
46
47
48
49
50
51
52
53
54
55
56
57
58
59
60